CHAPTER -III

HARMONIC OSCILLATORS REALISED WITH OTAs

3.1 INTRODUCTION

OTA-C oscillators offer many attractive features as compared to conventional op-amp based oscillators. They have now become increasingly important in view of their adaptability for implementing high frequency digitally programmable sinusoidal oscillators in CMOS technology [1].

The current interest towards searching for more and more efficient OTA-based sinusoidal oscillator circuits is motivated by the following possible advantages of OTA-based oscillators over conventional op-amp-based oscillators [2]:

(a) Linear electronic tunability of oscillation frequency Since the transconductance g_m, of an OTA is linearly controllable through an external amplifier bias current I_{ABC}, i.e.

$$g_m = \frac{I_{ABC}}{2V_T} \qquad (3.1.1)$$

the oscillation frequency f_o of OTA-based oscillators is normally given by an expression of the form

$$f_o = \frac{g_m}{2\pi C} \qquad (3.1.2)$$

and thus, providing $f_o \propto I_{ABC}$;

(b) Relatively higher operating frequency range; and

(c) Suitability for IC implementation: Since the internal circuit of an OTA may be designed with a very small number of resistors (or none at all), OTA oscillators are more suitable for IC implementation in any of the contemporary technologies used for fabricating analogue ICs (with bipolar OTAs in bipolar technology and with CMOS OTAs in MOS technology).

In the present chapter a brief review of some of the important works done on OTA-C oscillators has been present. Some of these oscillator circuits have been realised in hardware and the corresponding results have been presented.

3.2 LINEARLY TUNABLE WIEN BRIDGE OSCILLATOR REALISED WITH OPERATIONAL TRANSCONDUCTANCE AMPLIFIERS [2]

Senani and Kumar [2] presented an OTA-C sinusoidal oscillator which has been evolved from the classic Wien bridge oscillator (WBO). This circuit provides linear control of oscillation frequency through an external current signal. The circuit and its development methodology is described below.

The derivation of the present circuit starts from the op-amp-based Wien bridge oscillator (WBO) of Fig. 3.1(a), for which the conditions of oscillation and frequency of oscillation are known to be

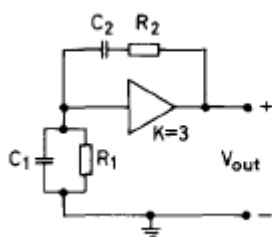$$K \geq 3 \qquad \text{With} \qquad C_1 = C_2 = C \qquad R_1 = R_2 = R$$

$$f_o = \frac{g_m}{2\pi RC} \tag{3.2.1}$$

A direct element-to-element OTA analogue is then obtained by simulating the grounded resistor R_1, floating resistor R_2, and the K-gain VCVS by appropriate OTA circuits. The resulting oscillator is shown in Fig.3.1 (c), and is characterised by
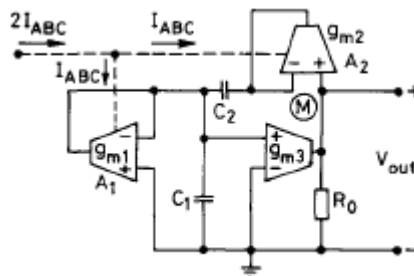
$$g_{m3} R_o = 3$$

$$f_o = \frac{g_m}{2\pi C}$$

$$\text{With} \quad C_1 = C_2 = C \qquad g_{m1} = g_{m2} = g_{m4} = g_m \tag{3.2.2}$$

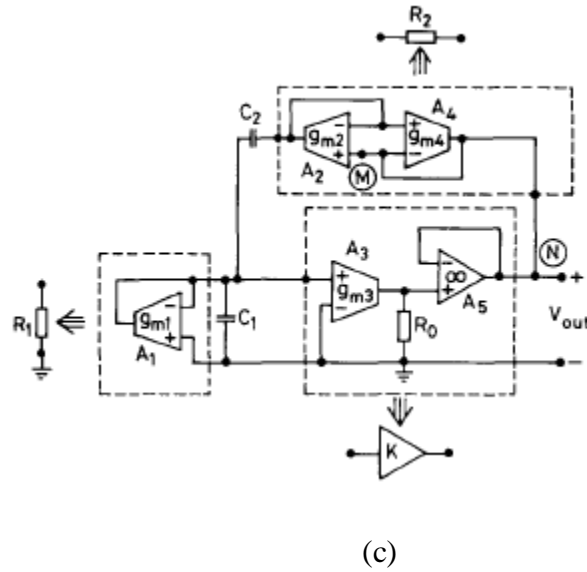(a)   (b)

(c)

Fig. 3.1 Derivation of new OTA-based oscillator circuit (a) Conventional Wien bridge oscillator (WBO) (b) Final simplified OTA-based WBO (c) Direct analogue of WBO in terms of OTAs [2].

3.3 GENERATION, DESIGN AND TUNING OF OTA-C HIGH-FREQUENCY SINUSOIDAL OSCILLATORS [3]

In [3] Linaress-Barranco, Rodriguez-Vazquez, Huertas and Sanchez-Sinencio have proposed a method described below generation, design and tuning of OTA-C high-frequency sinusoidal oscillators. Development of the circuit and its working is described below.

3.3.1 General TACO topology

The generation of TACOs is a particular example of the general circuit theoretical problem of synthesising a mathematical specification from a given reduced set of circuit components. In particular, the primitives for TACOS are capacitors and voltage controlled current sources (VCCSs), these latter components arising when modelling the OTA by circuit elements, as is shown in Fig. 3.2 for an ideal OTA model. Hence, the problem of synthesising a TACO reduces to that of approximately connecting such primitives to get a characteristic equation having a pair of complex roots on the imaginary axis and all the remaining roots on the left-half of the complex frequency plane.

Fig. 3.3 shows the general topology for an N-node TACO. The current sources in this Figure are multiple input VCCS described by

55

$$i_k = \sum_{j=1}^{N} g_{kj} v_j, \qquad\qquad 1 \le K \le N \qquad\qquad (3.3.1)$$

where g_{ij} is an arbitrary real-valued number and v_j is the voltage at the jth node. These multi-inputs grounded current sources can be readily implemented by connecting several OTA outputs in parallel.
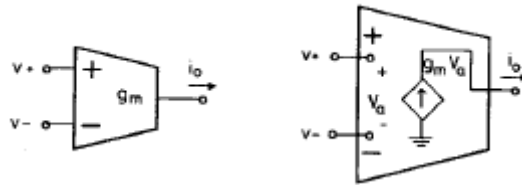

Fig. 3.2 Symbol and ideal model for OTA [3]

Nodal analysis allows us to write the following matrix equation for Fig. 3.3:

$$(G - sC)V_n(s) = 0 \qquad\qquad (3.3.2)$$

where $V_n^T = \{v_1, v_2, v_3, \dots\dots, v_N\}$, G is an N x N matrix containing the admittance description for the VCCSs and C is the N x N capacitance matrix for the network.

For the circuit of Fig. 3.3 to generate oscillations, eqn. 3.3.2 must exhibit a solution different from the trivial one, $V_n(s) = 0$. This yields the following characteristic equation for the general topology:

$$|G - sC| = 0 \qquad\qquad (3.3.3)$$

In the most general case, an Nth-order equation in the   complex frequency s results after calculating the matrix determinant in eqn. 3.3.3.
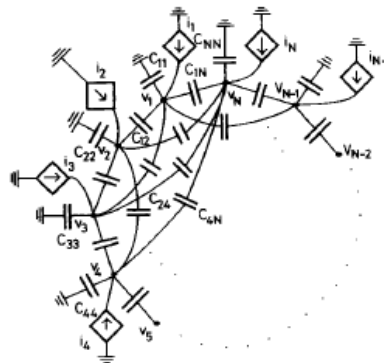

Fig. 3.3 General topology for generation of TACOS [3]

However, the order of the characteristic equation can be controlled by eliminating some of the current sources. As a matter of fact, matrix analysis allows us to conclude that the maximum order of the characteristic equation for a given topology coincides with the number of nonzero-valued current sources in Fig. 3.3.

The corresponding general expression for the characteristic equation of a second order oscillator is given by

$$s^2 - bs + \Omega_o^2 = 0 \tag{3.3.4}$$

Ideally, for oscillation b = 0. However, in practical oscillators and due to the influence of parasitics, the poles are displaced from their nominal positions at $s_p = \pm j\Omega_o$ to either the right-hand or the left-hand side of the complex frequency plane. For this reason, the oscillator must be designed to have its poles initially located inside the right-half complex frequency plane to assure a self starting operation, i.e. b ≥ ϵ, where E is a small positive number. Besides, nonlinearities have to be considered to explain the existence of stable oscillations [3].

In practical structures, b and Ω_o^2: in eqn. 3.3.4 are given as functions of the OTA transconductance gains and capacitor values. The basic TACO design goal is to achieve a separate control of these parameters with a minimum component count. For second-order oscillators, which need only two current sources in Fig. 3.3, several cases can be distinguished depending on the number of nodes in the circuit.

3.3.2 Two-node TACO topology [3]

Fig. 3.4 shows the conceptual circuit diagram for a two node TACO topology along with the expression for the VCCSs.

(a)
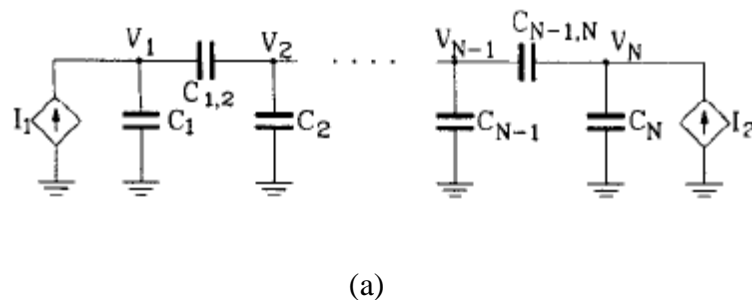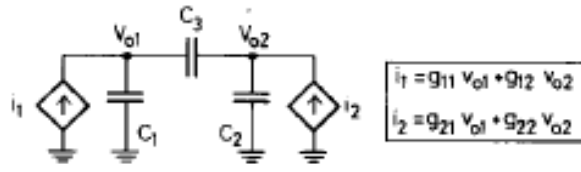
(b)

Fig. 3.4 (a) General topology for the generation of second-order OTA-C oscillators

(b) Conceptual circuit diagram for two-nodes TACO [3].

In this circuit, the Characteristic equation can be expressed as

$$C_{eq}^2 s^2 - s[g_{11}(C_2 + C_3) + g_{22}(C_1 + C_3) + (g_{12} + g_{21})C_3] + g_{11}g_{22} - g_{12}g_{21} = 0 \quad (3.3.5a)$$

where we define

$$C_{eq}^2 = C_1 C_2 + C_1 C_3 + C_2 C_3 \quad (3.3.5b)$$

(a) Two degrees of freedom:

Let us make $g_{11} = g_{22} = 0$ in eqn. 3.3.5. The following condition must apply for the characteristic equation to be appropriate for the generation of self starting sinusoidal oscillation ($\Omega_o^2 > 0$, b > 0):

$$sgn(g_{12}) \neq sgn(g_{21}); \quad (g_{12} + g_{21}) > 0 \quad (3.3.6)$$

Consider $g_{12} = g_{m1} > 0$, $g_{21} = -g_{m2} < 0$. Fig. 3.3.7 shows the corresponding TACO structure. Henceforth, we will refer to this structure as 2-OTA-3C. The characteristic equation for the 2-OTA-3C-TACO becomes

$$s^2 - s\frac{C_3}{C_{eq}^2}(g_{m1} - g_{m2}) + \frac{g_{m1}g_{m2}}{C_{eq}^2} = 0 \quad (3.3.7)$$

Parameter b depends on the difference between both transconductance gains whereas parameter Ω_o^2 depends on their product. Both design parameters can be trimmed by appropriately setting g_{m1} and g_{m2}. In this sense, we say that the circuit of Fig. 3.5 exlubits two degrees of freedom.
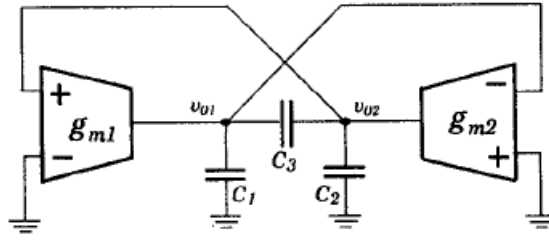
58

Fig. 3.5 2-OTA-3C oscillator structure[3]

(b) Three degrees of freedom:

The circuit of Fig. 3.3.7 is the simplest TACO that can be obtained by using an ideal OTA model. However, it exhibits a limitation in the interdependence between both design parameters b and Ω_o^2. Having independent control of these parameters would allow us to adjust the frequency of operation without affecting the oscillation condition, which is an appealing feature for VCO operation. Additional OTAs are required to achieve this. From eqn. 3.3.5 it can be seen that the simplest possibility is to make $g_{11} = g_{m3} > 0$, $g_{22} = 0$ and $C_3 = 0$, thereby resulting in the TACO structure of Fig. 3.6, henceforth called 3-OTA-2C. The characteristic equation for Fig. 3.6 is given by

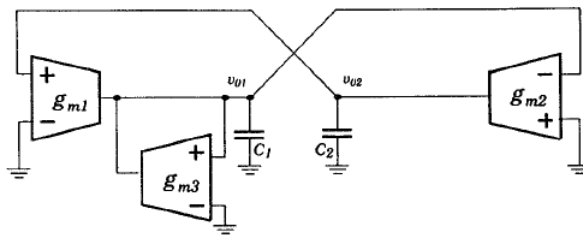$$s^2 - s\frac{g_{m3}}{C_1} + \frac{g_{m1}g_{m2}}{C_1 C_2} = 0 \qquad (3.3.8)$$

Fig 3.6 3-OTA-2C TAC oscillator structure [3]

It may be noted that parameter b is a linear function of the transconductance gain g_{m3}, while being independent of g_{m1} and g_{m2} . Thus, separate control of b and Ω_o^2: is achieved.

(c) Four degrees of freedom [3]:

There is a limitation of Fig. 3.6 in that b is proportional to g_{m3} and cannot be controlled by any other parameter. Because in practical designs b has to be made small enough to reduce

distortion, very small values of g_{m3} are required, which may cause the different OTAs in this TACO to work under very different bias conditions and voltage swings.

This problem is overcome by the structure shown in Fig. 3.7 (a), called 4-OTA-2C. Here we obtain

$$b = \frac{g_{m3}}{C_1} - \frac{g_{m4}}{C_2}; \qquad \Omega_o^2 = \frac{g_{m1}g_{m2} - g_{m3}g_{m4}}{C_1 C_2} \qquad (3.3.9a)$$

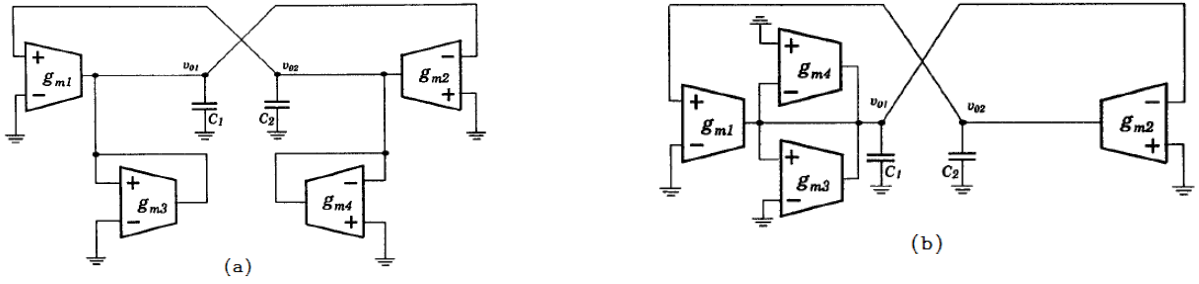where the possibility of independently adjusting b and Ω_o^2: can be observed.

Fig. 3.7 TACO structures (a) 4-OTA-2C TACO structure (b) Alternative 4-OTA-2C TACO structure
[3]

However, there is still a coupling between Ω_o^2: and b through g_{m3}, g_{m4}. This can be avoided by connecting g_{m4} to the same node as g_{m3} as shown in Fig. 3.7(b). In this case we get

$$b = \frac{g_{m3}}{C_1} - \frac{g_{m4}}{C_1}; \qquad \Omega_o^2 = \frac{g_{m1}g_{m2}}{C_1 C_2} \qquad (3.3.9b)$$

3.3.3 More than two node TACOS [3]

A lot of alternatives arise when trying to obtain new TACO structures from the general topology of Fig. 3.3. Our main purpose here is only reporting a reduced set of structures that can be practical. Consider, for this purpose, the four-node TACO of Fig. 3.8 (4-OTA-4C),

Which yields a second-order characteristic equation is given

$$b = \frac{g_{m3}}{C_3} - \frac{g_{m4}}{C_4};$$

$$\Omega_o^2 = \left\{ \frac{g_{m1}g_{m2}}{C_1 C_2} - \frac{g_{m3}g_{m4}}{(C_1+C_3)(C_2+C_4)} \right\} \times \left\{ \frac{(C_1+C_3)(C_2+C_4)}{C_3 C_4} \right\} \qquad (3.3.10)$$
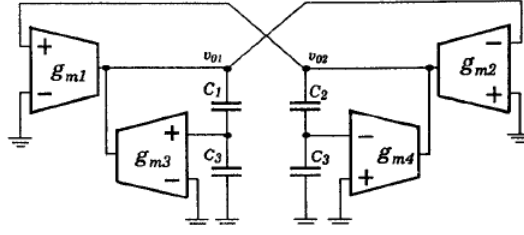
Fig. 3.8 4-OTA-4C TACO structure [3]

A difference between this new structure and both the 4-OTA-2C and quadrature can be observed in the way of controlling the design parameters via capacitor values. Here we can separately adjust both b and Ω_o^2 by using the capacitors C_1, C_2, C_3 and C_4. Specifically, note that decreasing the values of C_1, and C_2, results in an increased value of Ω_o^2: without affecting the value of b. It may be an appealing feature for low distortion high-frequency operation. Besides, in monolithic implementation, choosing $(C_3, C_4) > (C_1, C_2)$ means that the parasitic capacitor at the bottom plates of both C_1 and C_2 are negligible as compared to C_3 , C_4 .

TABLE 3.1

Ideal Expression of b_c and Ω_0^2 for Different TACO Structure

$(g_{m1} - g_{m2})C_3$	b_c	
$\dfrac{g_{m1}g_{m2}}{(C_1 + C_3)(C_2 + C_3) - C_3^2}$	Ω_{0c}^2	2-OTA-3C
$(g_{m3}C_2 - g_{m4}C_1)$	b_c	
$\dfrac{g_{m1}g_{m2} - g_{m3}g_{m4}}{C_1 C_2}$	Ω_{0c}^2	4-OTA-2C
$(g_{m3} - g_{m4})C_2$	b_c	
$\dfrac{g_{m1}g_{m2}}{C_1 C_2}$	Ω_{0c}^2	Quadrature
$(g_3 - g_4)\dfrac{C_1 C_2 C_3}{(C_1 + C_3)(C_2 + C_3)}$	b_c	
$\dfrac{g_{m1}g_{m2}\left(1 + \dfrac{C_1}{C_3}\right)\left(1 + \dfrac{C_2}{C_3}\right) - g_{m3}g_{m4}\dfrac{C_1 C_2}{C_3^2}}{C_1 C_2}$	Ω_{0c}^2	4-OTA-4C

3.4 GENERATION OF NEW OTA-C OSCILLATOR STRUCTURES USING NETWORK TRANSPOSITION [4]

A simple but very useful approach based on network transposition principle has been presented by Swamy, Raut and Tang in [4] and is described below to derive new CMOS sinusoidal oscillators using operational transconductance amplifiers and capacitors (OTA-C). The principle of mirroring to convert a three-terminal two-port network to a four-terminal fully differential network is utilized to generate fully differential OTA-C oscillator structures. The theoretical work is verified by using discrete resistors, capacitors and OTA devices.

3.4.1 A brief review of network transposition

It is known that given a linear network N, its transposed network N_T can be directly obtained by simply replacing the nonreciprocal elements by their corresponding transposes and leaving the reciprocal elements unchanged. In such a case, the voltage transfer function (VTF) of N in the forward direction is the same as the current transfer function (CTF) of N_T in the reverse direction and vice versa . In terms of practical application, using network transposition a current mode OTA-C filter structure can be obtained in a straightforward manner from a voltage mode OTA-C filter by simply interchanging the input and output terminals of each OTA and reversing the input and output ports of the filter . It is also known that the original and the transposed network would have identical transfer functions and sensitivities with respect to the corresponding parameters.

3.4.2 Transposition and OTA-C oscillators [4]

Let N and N_T be two second-order three-terminal active networks as shown in Fig. 3.9 with transfer functions is

$$(V_o/V_i) = (I_o/I_i) = a\,(s^2 - ds + e)/(s^2 - bs + c) \tag{3.4.1}$$

The characteristic equation (CE) of N is the same as that of N_T,

$$s^2 - bs + c = 0 \tag{3.4.2}$$

For network N, if $V_i = O$ and the voltage source V_i is replaced, by its zero internal impedance leaving the output terminals open, N assumes the basic structure of an oscillator (say, oscillator A) as shown in Fig. 3.10(a). Similarly, for the network N_T if $I_i = O$ and the current source I_i, is

replaced by its infinite internal impedance, N_T assumes the basic structure of the transposed oscillator (say oscillator B) as shown in Fig. 3.10(b). The CE in either of the cases is the same and is given by (1). Thus, another oscillator structure B can be derived from the original oscillator by network transposition. To ensure that oscillation exists, be stable and unique, the condition of oscillation $b=O$ should be satisfied and c that determines the frequency of oscillation must be greater than 0. The original oscillator A and the transposed one, oscillator B, have the same CE as well as the same condition and frequency of oscillation. Also, the various sensitivities with respect to the corresponding parameters are identical. Thus, the two oscillators are expected to have similar performances.

3.4.3 Single output oscillator structures [4]

Several OTA-C oscillator architectures employing single output OTAs and capacitors have been proposed in the past. Based on these architectures, new transposed OTA-C oscillator architectures can be obtained by the application of network transposition. For example, consider the OTA-C oscillator shown in Fig. 3.11(a) . At first, it is treated as a VM filter, whose VTF (V_o/V_i) is given by

$$(s^2 C_1 C_2)/\{s^2 C_1 C_2 - s(g_{m1}C_2 - g_{m2}C_1) + g_{m1}g_{m2}\} \qquad (3.4.3)$$

By applying network transposition, we can derive the corresponding CM filter, as shown in Fig. 3.11(b) with its CTF (I_o/I_i) given by

$$(s^2 C_1 C_2)/\{s^2 C_1 C_2 - s(g_{m1}C_2 - g_{m2}C_1) + g_{m1}g_{m2}\} \qquad (3.4.4)$$

As expected, both the filters have the same CE, namely,

$$s^2 C_1 C_2 - s(g_{m1}C_2 - g_{m2}C_1) + g_{m1}g_{m2} = 0 \qquad (3.4.5)$$

Now if $V_i=O$ for the VM filter and $I_i=O$ for the CM filter then both the networks function as oscillators as long as the condition of oscillation is satisfied: $b=O$, that is $g_{m1}C_2 = g_{m2}C_1$. also the frequency of oscillation for either of the oscillators is given by $(g_{m1}g_{m2}/C_1C_2)^{1/2}$.

3.4.4 Fully Differential Oscillator Structure [4]

Differential structures are widely used in OTA-C based designs because of improved common-mode rejection ratio, elimination of even-order harmonic distortion components, reduction of

the effects of power supply noise and increase in the output swing. Differential structures can be obtained from single-ended structures using the principle of mirroring. As an example, the differential oscillator configuration obtained from table s.no. 1 by using the principle of "mirroring" is shown in Fig. 12.
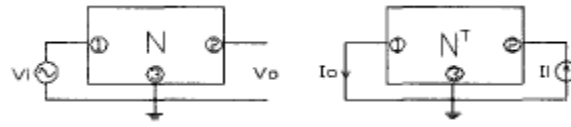

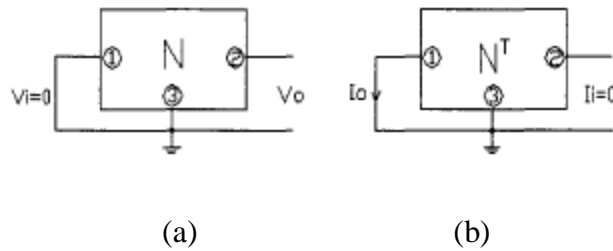Fig. 3.9 Second-order three-terminal active networks [4]

(a)   (b)
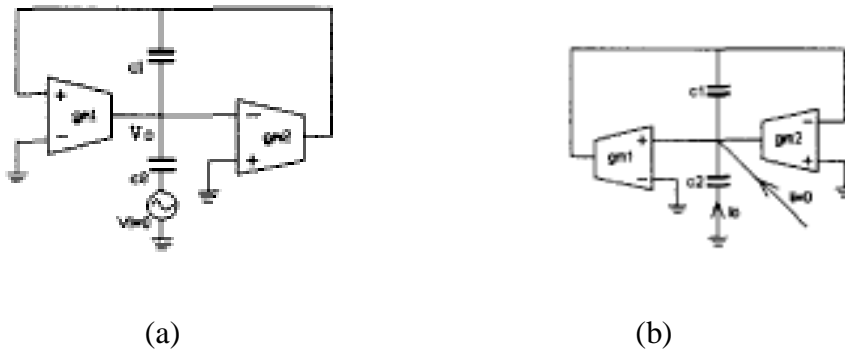
Fig. 3.10 (a) Oscillator A (b) Oscillator B [4]

(a)   (b)

Fig. 3.11 (a) Oscillator structure (b) Its transpose same as the (a) [4]
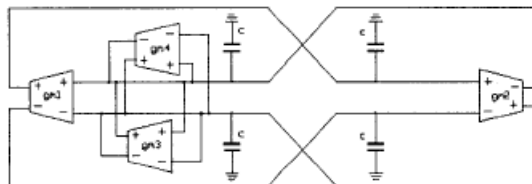
Fig. 3.12 Differential OTA-C oscillator [4]

3.5 NEW ELECTRONICALLY TUNABLE OTA-C SINUSOIDAL OSCILLATOR [5]

A new transconductance-amplifier-capacitor sinusoidal oscillator configuration was introduced in [5] by Senani which requires only three OTAs to facilitate generation of linearly tunable (through an external current or voltage) variable frequency oscillations. The circuit and its operation is described below.
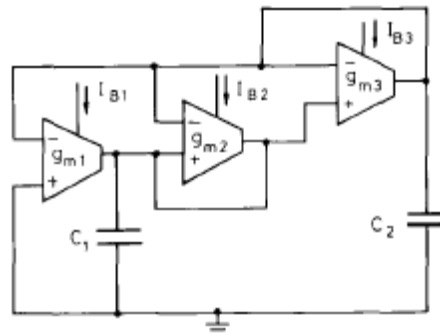
Fig. 3.13 TAC sinusoidal oscillator [5]

The circuit is shown in Fig. 3.13. By routine analysis, the condition of oscillation is found to be

$$g_{m3} - g_{m2} = 0 \quad \text{with} \quad C_1 = C_2 = C \tag{3.5.1}$$

Where as the frequency of oscillation is given by

$$f_o = \frac{1}{2\pi C}\sqrt{(g_{m1}g_{m2})} \tag{3.5.2}$$

If the transconductances of the three OTAs are varied simultaneously through a single external current I_B, then

$$g_{m1} = g_{m2} = g_{m3} = g_m \tag{3.5.3}$$

and consequently, eqn. 3.5.2 reduces to

$$f_o = \frac{g_m}{2\pi C} \tag{3.5.4}$$

Since

$$g_{mi} = \frac{I_{Bi}}{2V_T} \quad \text{i=1-3}$$

eqn. 3.5.4 becomes

65

$$f_o = \frac{I_B}{4\pi C V_T} \qquad\qquad (3.5.5)$$

Thus, fo is linearly controllable through an external current signal I_B, without disturbing the condition of oscillation which always remains satisfied in view of eqn. 3.5.3.

3.6 DIGITALLY PROGRAMMABLE ACTIVE-C OTA-BASED OSCILLATOR [6]

In [6] Abuelma'atti and Almaskati have presented a novel active-C OTA-based oscillator circuit. The circuit enjoys noninteractive electronic tunability, uses the minimum number of active and passive components, and enjoys low sensitivity characteristics. The frequency of oscillation can be digitally controlled and the circuit can he easily interfaced with mini-microcomputer- or microprocessor-based systems.The circuit and its working is described in the following.

3.6.1 Oscillator circuit

Consider the circuit shown in Fig. 3.14. Assuming ideal OTA's. routine analysis yields the characteristic equation of the circuit given by

$$S^2 C_1 C_3 + S[(G_2 - g_2)(C_1 + C_3)] + g_1(g_2 - G_2) = 0 \qquad\qquad (3.6.1)$$

where G_2 represents the input resistance of the OTA,. By equating the real and imaginary parts of (1) to zero, the frequency of oscillation and the condition of oscillation will be given by

$$\omega_o = \sqrt{\frac{g_1(g_2 - G_2)}{C_1 C_3}} \qquad\qquad (3.6.2)$$

And
$$g_2 = G_2 \qquad\qquad (3.6.3)$$
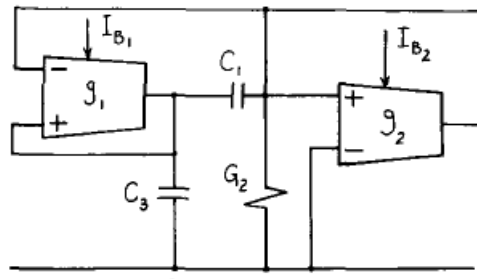
Fig 3.14. Oscillator circuit Proposed in [6].

From (3.6.2), (3.6.3) it is obvious that the frequency of oscillation can be changed by adjusting gl without affecting the condition of oscillation, i.e., the circuit enjoys noninteractive electronic tunability. Moreover, since the frequency of oscillation is a function of g_1 which in turn is a function of the dc-bias current I_{B1}, then by obtaining I,, from the output of a digital-to-analog converter (DAC), the realization of a digitally-programmable electronically-tunable oscillator is feasible.

3.7 SYSTEMATIC DERIVATION OF ALL POSSIBLE CANONIC OTA-C SINUSOIDAL OSCILLATORS [7]

In [7] Bhaskar, Tripathi, and Senani, have presented a systematic derivation of all possible canonic OTA-C sinusoidal oscillators. The method is presented below.

There are only five possibilities in which two capacitors can be embedded in an all OTA network N (denoted as N_a - N_e in fig.3.15).
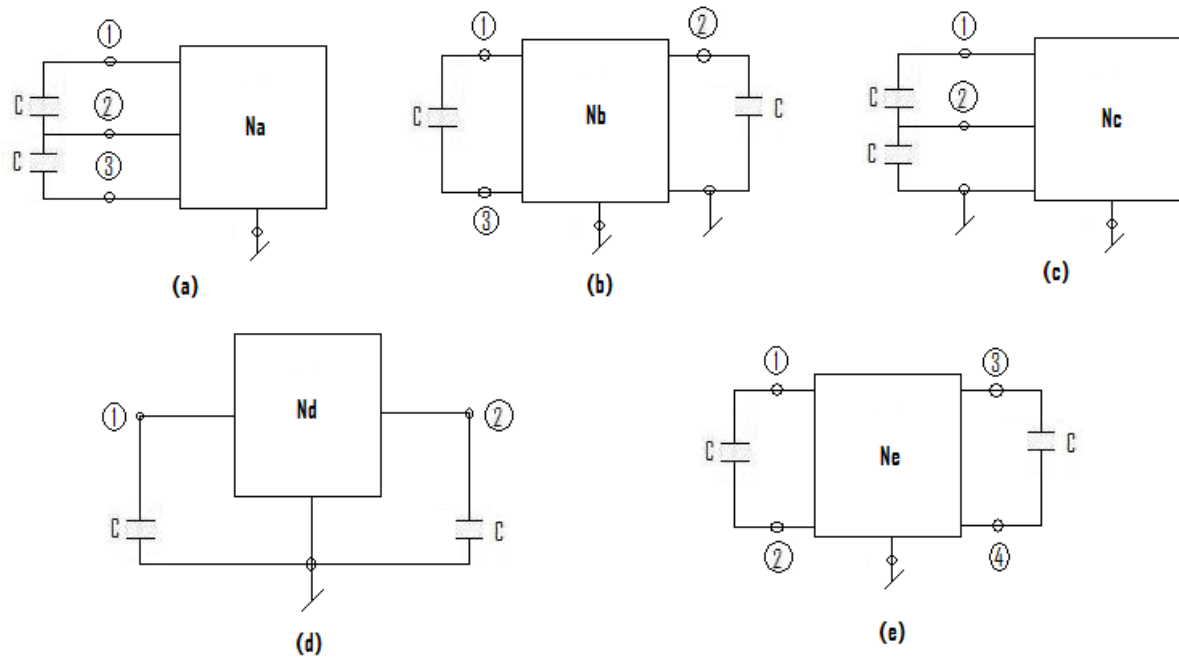
Fig 3.15 Five possible structures for the synthesis of canonic OTA-C sinusoidal oscillators [7].

The general form of the characteristic equation (CE) of all the oscillators, based on any of these five structures, would be of the form:

$$s^2 + b_1 s + b_0 = 0 \tag{3.7.1}$$

It is easy to see that the frequency of oscillation f_0 given by $f_0 = (b_0)^{1/2}$ can have correct dimensions by being dependent on only two of the transconductances of the OTAs contained in the networks N_a - N_e, thus, leading to the expression for f_0 of the type

$$f_0 = \frac{1}{2\pi C}[g_1 g_2]^{1/2} \tag{3.7.2}$$

(Assuming for simplicity $C_1 = C_2 = C$).

To make the oscillator self-starting, the roots of CE must be movable in the right half of the s-plane (for building up the oscillations) and on the $\pm j\omega$ axis (for facilitating sustained oscillations). This, in turn, means that the coefficient b_1 in the CE should contain a difference of two transconductances in either of the two possible forms:

$$b_1 = \pm(g_1 - g_3)C \quad \text{or} \quad \pm(g_2 - g_3)C \tag{3.7.3}$$

$$b_1 = \pm(g_3 - g_4)C \tag{3.7.4}$$

It is to be noted that in both of these cases f_0 can be independently controlled without affecting the condition of oscillation (CO). Also, the oscillators having characterizations (3.7.2) and (3.7.4) would require at least four OTAs whereas those characterized by (3.7.2) and (3.7.3) should be realizable with only three OTAs. Therefore, the minimum number of OTAs, for a canonic realization of an oscillator with non-interacting control of the FO, is three. Hence, in the formulation that follows we will be focusing on the realizations requiring only three OTAs and two capacitors.

3.7.1 Generation of canonic OTA-C sinusoidal oscillators

If the networks N_a-N_d are characterized by the short circuit admittance parameters, the CE for these cases turns out to be of the form (1) from where the CO and FO are found to be as follows.

Case (a)

$$\left[\left\{Y_{11} - \frac{(Y_{11}+Y_{12}+Y_{13})(Y_{11}+Y_{21}+Y_{31})}{Y_1}\right\} + \left\{Y_{33} - \frac{(Y_{13}+Y_{23}+Y_{33})(Y_{31}+Y_{32}+Y_{33})}{Y_1}\right\}\right] \leq 0$$

(3.7.5)

$$f_0 = \frac{1}{2\pi C}\left(\frac{det\,[Y_a]}{Y_1}\right)^{1/2}$$

(3.7.6)

Where

$$det[Y_a] = Y_{11}(Y_{22}Y_{33} - Y_{23}Y_{32}) - Y_{12}(Y_{21}Y_{33} - Y_{23}Y_{31}) + Y_{13}(Y_{21}Y_{32} - Y_{22}Y_{31})$$

(3.7.7)

$$Y_1 = Y_{11} + Y_{12} + Y_{13} + Y_{21} + Y_{22} + Y_{23} + Y_{31} + Y_{32} + Y_{33}$$

(3.7.8)

Case (b)

$$\left[\left\{Y_{11} - \frac{(Y_{11}+Y_{31})(Y_{11}+Y_{13})}{Y_2}\right\} + \left\{Y_{22} - \frac{(Y_{12}+Y_{32})(Y_{21}+Y_{23})}{Y_2}\right\}\right] \leq 0$$

(3.7.9)

$$f_0 = \frac{1}{2\pi C}\left(\frac{det\,[Y_b]}{Y_2}\right)^{1/2}$$

(3.7.10)

Where

$$det[Y_b] = det[Y_a]$$

(3.7.11)

$$Y_2 = (Y_{11} + Y_{13} + Y_{31} + Y_{33})$$

(3.7.12)

Case (c)

$$[2Y_{11} + Y_{12} + Y_{21} + Y_{22}] \leq 0$$

(3.7.13)

$$f_0 = \frac{1}{2\pi C}\,(det[Y_c])^{1/2}$$

(3.7.14)

Where

$$det[Y_c] = (Y_{11}Y_{22} - Y_{12}Y_{21})$$

(3.7.15)

Case (d)

$$[Y_{11} + Y_{22}] \leq 0$$

(3.7.16)

$$f_0 = \frac{1}{2\pi C}\,(det[Y_d])^{1/2}$$

(3.7.17)

Where
$$det[Y_d] = det[Y_c] \qquad (3.7.18)$$

An inspection of the above equations suggests that in order to have the oscillators based upon networks N_a-N_e with no more than three OTAs, a number of elements in the Y-matrix characterization would have to be selected as zeros. The selection of such zero entries (ZE), however, cannot be made arbitrarily in view of the following restrictions applicable to all of the cases being considered here.

Restriction 1

All elements in any row cannot be simultaneously zero because this makes the corresponding port current zero (thereby making one capacitor in the circuit redundant).

Also, in such a case $det[Y_j]$ (j = a-e) becomes zero and hence $f_o = 0$.

Restriction 2

 All elements in any column cannot be simultaneously zero as this also makes

$det[Y_j]$ (j = a-e) becomes zero and hence $f_o = 0$.

The various feasible cases may now be examined in detail. While synthesizing the three-OTA oscillators of the desired kind as set out in the previous section, it will be shown that apart from the tuning laws of the form (3.7.2) and (3.7.3) there are many other forms of tuning laws, the three OTA oscillators corresponding to which can provide independent control of the FO.

Restriction 3

If the zeros are distributed one in each row, then in order to have a three-OTA structure each row must have remaining two entries equal and opposite (i.e. all three OTAs to be connected in differential mode). Such a situation makes $det[Y] = 0$ and hence FO becomes zero.

Restriction 4

If zero are distributed such that one row does not contain any ZE (this row will then have three transconductances and would require at least two OTAs), one row contains one ZE and the rest two zeros appear in the remaining row, then the resulting matrix cannot be realized with only three OTAs.

Thus, any $[Y]$ matrix characterization having only three ZEs cannot result in a three-OTA structure of the desired type.

Case a :-

OTA-C oscillators employing two floating capacitors with a common node: In view of the restriction 1 and 2, the possibility of three zeros lying in any single row or single column is ruled out. The other possibilities may now be considered.

 (i) Three ZEs in $[Y_a]$.
 (ii) Four ZEs in $[Y_a]$

This implies that OTA circuit corresponding to this would have two OTAs in differential mode and the third OTA in single ended mode. Although four entries can be selected out of nine in $(9!/4!5!) = 126$ ways, the only meaningful ways are those(keeping in mind restriction 1,2 and 3 as outlined above) where out of the four ZEs two row contain one ZE and a third row contains two ZEs. The total number of possible cases having this kind of assignment of ZEs turn out to be 63. The resulting 63 characterizations of $[Y_a]$ are then checked to find which of these result in three- OTA oscillators possessing independent control of FO. It has been found that none of this set of 63 characterizations of $[Y_a]$ results in any oscillator of the desired type.

(iii) Five ZEs in $[Y_a]$

This implies that OTA circuit corresponding to this would have one OTAs in differential mode and the two OTAs in single ended mode. On the basis of the considerations

Similar to those outlined in (i) and (ii), the total number of possible characterizations corresponding to this case is 45 out of which only 16 qualify to yield three-OTA oscillators of the desired kind. Further, if port transposition is applied , the number of oscillator circuits reduces to eight. These are shown in Table 3.3.
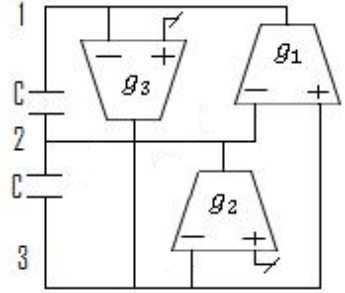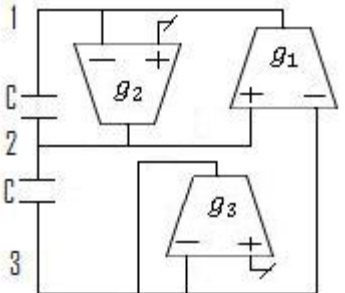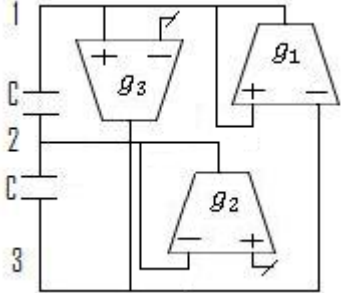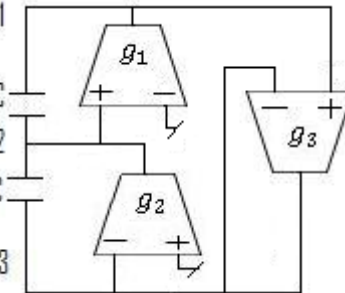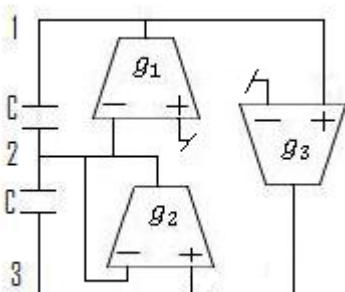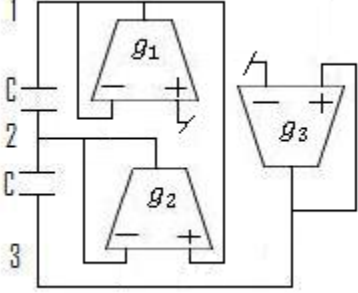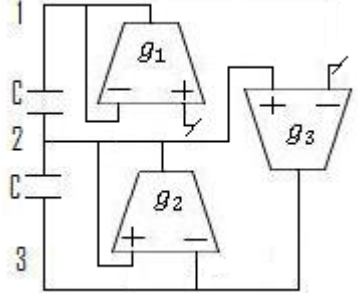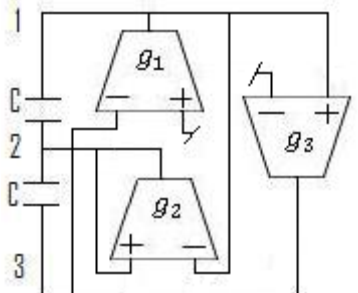
(iv) Six ZEs in $[Y_a]$

This implies that all three OTAs are to be connected ina single ended mode. It is obvious that each row should have one and only one transconductance and, therefore, keeping in mind restrictions 1 and 2, the total number of characterizations of interest are only six in this case. None of these, however, result in oscillators providing independent contro of FO.

The possibility of having more than six ZEs and less three ZEs in $[Y_a]$ is ruled out; the former because of resulting in the $[Y_a]$ matrix not permissible due to restriction 1 and 2, the latter because of the reqirement of more than three OTAs.

TABLE 3.3

Various oscillator realizations corresponding to schematic of Fig. 3.15(a)

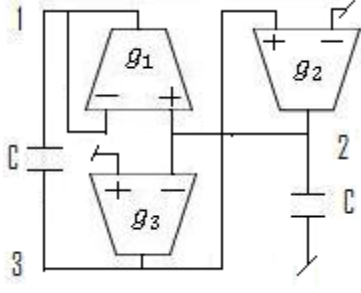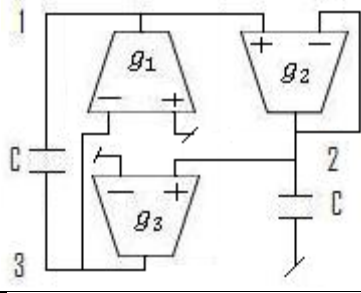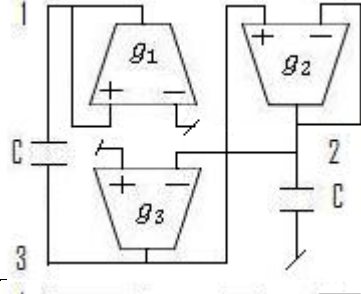| S.No.	Generic $[Y]$ matrix	Oscillator circuit	CO and FO
1.	$\begin{bmatrix} 0 & g_1 & -g_1 \\ 0 & 0 & g_2 \\ g_3 & 0 & 0 \end{bmatrix}$		$(g_1 - g_2) = 0$ $f_0 = \frac{1}{2\pi C} \sqrt{\frac{g_1 g_2 g_3}{g_2 + g_3}}$
2.	$\begin{bmatrix} 0 & -g_1 & g_1 \\ g_2 & 0 & 0 \\ 0 & 0 & g_3 \end{bmatrix}$		$(g_2 - g_1) = 0$ $f_o = \frac{1}{2\pi C} \sqrt{\frac{g_1 g_2 g_3}{g_2 + g_3}}$
3.	$\begin{bmatrix} -g_1 & 0 & g_1 \\ 0 & g_2 & 0 \\ -g_3 & 0 & 0 \end{bmatrix}$		$(2g_3 - g_2) = 0$ $f_o = \frac{1}{2\pi C} \sqrt{g_1 g_2}$
4.	$\begin{bmatrix} 0 & -g_1 & 0 \\ 0 & 0 & g_2 \\ -g_3 & 0 & g_3 \end{bmatrix}$		$(g_2 - 2g_1) = 0$ $f_o = \frac{1}{2\pi C} \sqrt{g_2 g_3}$
5.	$\begin{bmatrix} 0 & g_1 & 0 \\ 0 & g_2 & -g_2 \\ -g_3 & 0 & 0 \end{bmatrix}$		$(g_1 - g_2) = 0$ $f_o = \frac{1}{2\pi C} \sqrt{\frac{g_1 g_2 g_3}{g_1 - g_3}}$ $g_3 < g_1$

6.	$\begin{bmatrix} g_1 & 0 & 0 \\ -g_2 & g_2 & 0 \\ 0 & 0 & -g_3 \end{bmatrix}$		$(-g_2 + 2g_3) = 0$ $f_o = \dfrac{1}{2\pi C}\sqrt{\dfrac{g_1 g_2 g_3}{g_3 - g_1}}$ $g_1 < g_3$
7.	$\begin{bmatrix} g_1 & 0 & 0 \\ 0 & -g_2 & g_2 \\ 0 & -g_3 & 0 \end{bmatrix}$		$(g_2 - g_1) = 0$ $f_o = \dfrac{1}{2\pi C}\sqrt{\dfrac{g_1 g_2 g_3}{g_1 - g_3}}$ $g_3 < g_1$
8.	$\begin{bmatrix} 0 & 0 & g_1 \\ g_2 & -g_2 & 0 \\ -g_3 & 0 & 0 \end{bmatrix}$		$(-2g_3 + g_2) = 0$ $f_o = \dfrac{1}{2\pi C}\sqrt{\dfrac{g_1 g_2 g_3}{g_3 - g_1}}$ $g_1 < g_3$

Case b:-
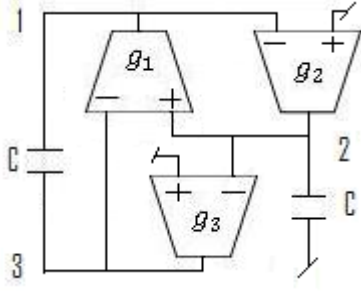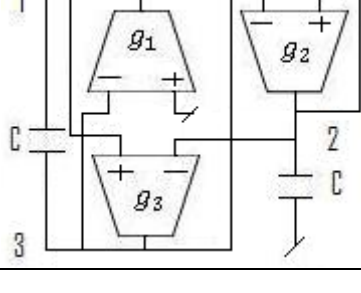
OTA-C oscillators employing one floating and one grounded capacitor having no common node: Since $[Y_b]$ is also 3×3 matrix like $[Y_a]$, the various constraints and restrictions on selecting ZEs, to arrive at three-OTA oscillator structures of the desired kind, are analogous to those for case (a). It has been found that:
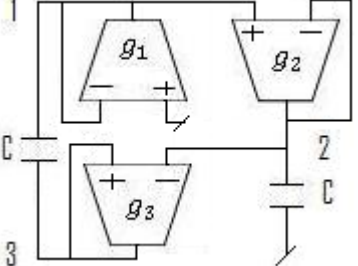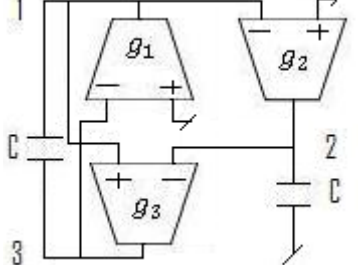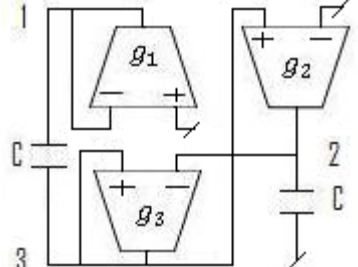
- Only four oscillators of the desired kind result from the 63 possibilities of selecting four ZEs;

- Only 12 oscillators of the desired kind result from the 45 possibilities of selecting five ZEs;

- The cases of three ZEs and six ZEs do not yield any valid realizations.

The various feasible oscillators (after deleting the redundant cases related by port-transposition) corresponding to this case are shown in Table 3.4.

TABLE 3.4

Various oscillator realizations corresponding to schematic of Fig. 3.15(b)

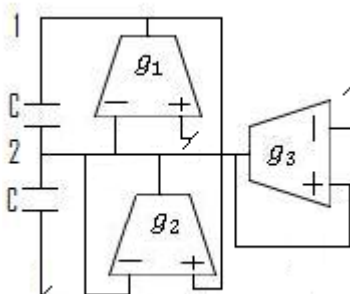| S.No..	Generic $[Y]$ matrix	Oscillator circuit	CO and FO
1.	$\begin{bmatrix} 0 & -g_1 & g_1 \\ g_2 & 0 & 0 \\ 0 & g_3 & 0 \end{bmatrix}$		$(-g_3 + g_1) = 0$ $f_o = \dfrac{1}{2\pi C}\sqrt{g_2 g_3}$
2.	$\begin{bmatrix} g_1 & -g_1 & 0 \\ 0 & 0 & -g_2 \\ 0 & g_3 & 0 \end{bmatrix}$		$(-g_1 + g_3) = 0$ $f_o = \dfrac{1}{2\pi C}\sqrt{g_2 g_3}$
3.	$\begin{bmatrix} 0 & 0 & g_1 \\ -g_2 & g_2 & 0 \\ 0 & -g_3 & 0 \end{bmatrix}$		$(-g_3 + g_1) = 0$ $f_o = \dfrac{1}{2\pi C}\sqrt{g_2 g_3}$
4.	$\begin{bmatrix} -g_1 & 0 & 0 \\ 0 & g_2 & -g_2 \\ 0 & g_3 & 0 \end{bmatrix}$		$(-g_3 + g_1) = 0$ $f_o = \dfrac{1}{2\pi C}\sqrt{g_2 g_3}$
5.	$\begin{bmatrix} 0 & 0 & g_1 \\ 0 & -g_2 & g_2 \\ -g_3 & g_3 & 0 \end{bmatrix}$		$(-g_2 + g_3) = 0$ $f_o = \dfrac{1}{2\pi C}\sqrt{\dfrac{g_1 g_2 g_3}{g_3 - g_1}}$ $g_1 < g_3$

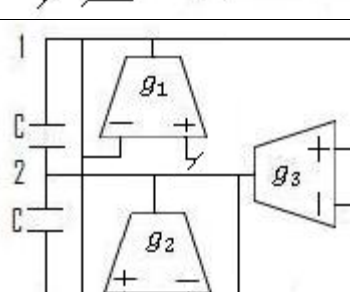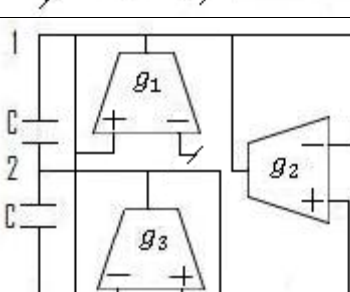|			
6.	$\begin{bmatrix} g_1 & 0 & 0 \\ -g_2 & g_2 & 0 \\ 0 & g_3 & -g_3 \end{bmatrix}$		$(g_2 - g_3) = 0$ $f_o = \dfrac{1}{2\pi C}\sqrt{\dfrac{g_1 g_2 g_3}{g_3 - g_1}}$ $g_1 < g_3$
7.	$\begin{bmatrix} 0 & 0 & g_1 \\ g_2 & 0 & 0 \\ -g_3 & g_3 & 0 \end{bmatrix}$		$(g_1 - g_2) = 0$ $f_o = \dfrac{1}{2\pi C}\sqrt{\dfrac{g_1 g_2 g_3}{g_1 - g_3}}$ $g_3 < g_1$
8.	$\begin{bmatrix} g_1 & 0 & 0 \\ 0 & 0 & -g_2 \\ 0 & g_3 & -g_3 \end{bmatrix}$		$(g_2 - g_1) = 0$ $f_o = \dfrac{1}{2\pi C}\sqrt{\dfrac{g_1 g_2 g_3}{g_1 - g_3}}$ $g_3 < g_1$

Case c:-
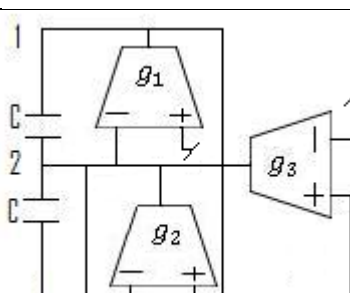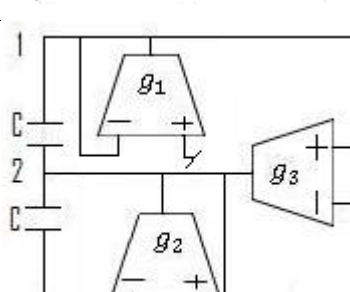
OTA-C oscillators employing one floating and one grounded capacitor having a common node: In this case, because N_c is a two port network and in view of the restrictions 1 and 2, at the most one element can be made zero out of the four elements in order to realize the desired type of oscillators. Thus, the following two possibilities should be considered:
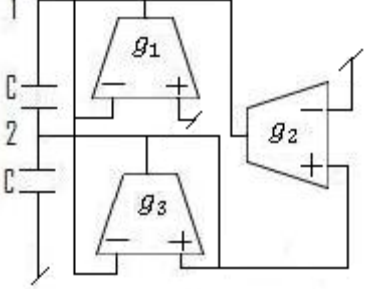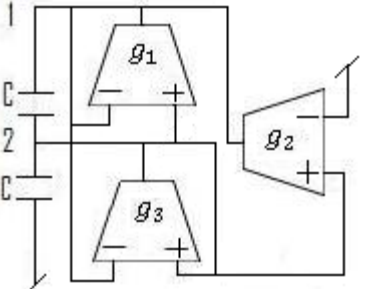
(i) one ZE in $[Y_c]$;

(ii) no ZE in $[Y_c]$.

A rigorous search for all possible choices of the elements of $[Y_c]$ which satisfy the CO and the FO has been made for both of the above cases. It turns out that only three distinctly different choices are possible for case (i), and four distinctly different combinations exist for the case (ii). The resulting $[Y_c]$ matrix and the oscillators corresponding to these are shown in Table 3.5.

TABLE 3.5

Various oscillator realizations corresponding to schematic of Fig. 3.15(c)

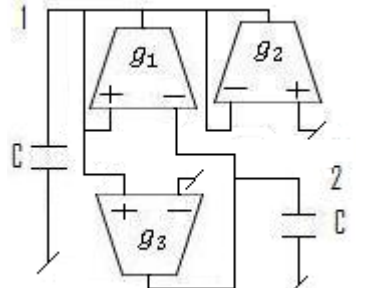| S.No.	Generic $[Y]$ matrix	Oscillator circuit	CO and FO
1.	$\begin{bmatrix} 0 & g_1 \\ -g_2 & g_2 - g_3 \end{bmatrix}$		$(g_1 - g_3) = 0$ $f_o = \dfrac{1}{2\pi C}\sqrt{g_1 g_2}$
2.	$\begin{bmatrix} 0 & g_1 \\ -g_2 - g_3 & g_2 \end{bmatrix}$		$(g_1 - g_3) = 0$ $f_o = \dfrac{1}{2\pi C}\sqrt{g_1(g_2 + g_3)}$
3.	$\begin{bmatrix} g_1 & 0 \\ -g_3 & g_3 - g_2 \end{bmatrix}$		$(2g_1 - g_2) = 0$ $f_o = \dfrac{1}{2\pi C}\sqrt{g_1(g_3 - g_2)}$ $g_2 < g_3$
4.	$\begin{bmatrix} g_1 & 0 \\ -g_2 - g_3 & g_3 \end{bmatrix}$		$(2g_1 - g_2) = 0$ $f_o = \dfrac{1}{2\pi C}\sqrt{g_1 g_3}$
5.	$\begin{bmatrix} -g_1 + g_2 & -g_2 \\ g_3 & -g_3 \end{bmatrix}$		$(-2g_1 + g_2) = 0$ $f_o = \dfrac{1}{2\pi C}\sqrt{g_1 g_3}$

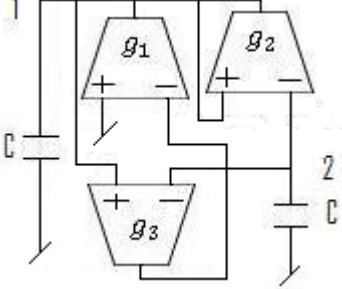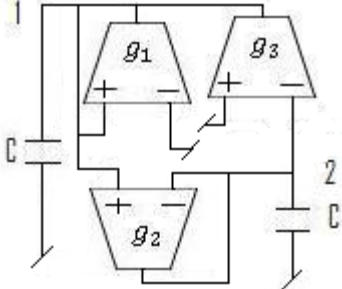| S.No.	Generic $[Y]$ matrix	Oscillator circuit	CO and FO
6.	$\begin{bmatrix} g_1 & -g_2 \\ g_3 & -g_3 \end{bmatrix}$		$(2g_1 - g_2) = 0$ $f_o = \dfrac{1}{2\pi C}\sqrt{g_1 g_3}$
7.	$\begin{bmatrix} g_1 & -g_1 - g_2 \\ g_3 & -g_3 \end{bmatrix}$		$(g_1 - g_2) = 0$ $f_o = \dfrac{1}{2\pi C}\sqrt{g_2 g_3}$

Case d:-

OTA-C oscillators with both the capacitors grounded. Since $[Y_d]$ is a 2×2 matrix like $[Y_c]$, the considerations to select appropriate entries for $[Y_d]$ are simiar to those of case (c). There are only three distinct forms of the matrix $[Y_d]$ which yield three-OTA oscillators of the desired kind. These generic matrices and the corresponding circuits are shown in Table 3.6.

TABLE 3.6

Various oscillator realizations corresponding to schematic of Fig. 3.15(d)

S.No.	Generic $[Y]$ matrix	Oscillator circuit	CO and FO
1.	$\begin{bmatrix} g_2 - g_1 & g_1 \\ -g_3 & 0 \end{bmatrix}$		$(g_2 - g_1) = 0$ $f_o = \dfrac{1}{2\pi C}\sqrt{g_1 g_3}$

2.	$\begin{bmatrix} -g_2 & g_1+g_2 \\ -g_3 & g_3 \end{bmatrix}$		$(g_3 - g_2) = 0$ $f_o = \dfrac{1}{2\pi C}\sqrt{g_1 g_3}$
3.	$\begin{bmatrix} -g_1 & g_3 \\ -g_2 & g_2 \end{bmatrix}$		$(g_2 - g_1) = 0$ $f_o = \dfrac{1}{2\pi C}\sqrt{g_2(g_3 - g_1)}$ $g_1 < g_3$

3.8 SAMPLE EXPERIMENTAL RESULTS

The workability of all the circuits of Tables 3.3-3.6 has been checked experimentally using CA 3080 type IC OTAs biased with the biasing arrangement shown below in Figure 3.16.
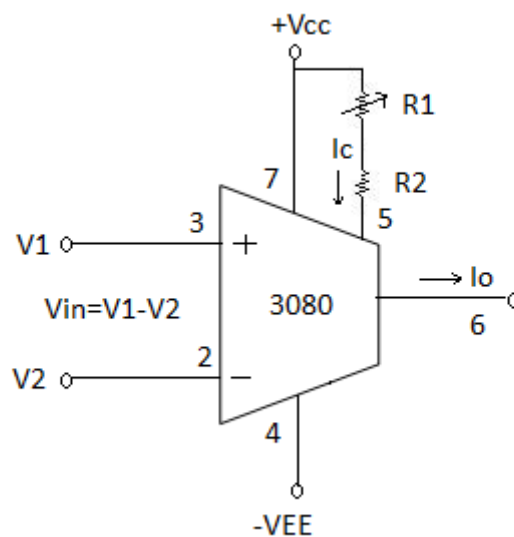
Fig. 3.16 Schematic of CA3080 OTA

Some sample experimental results from the structures of table 3.3-3.6 are shown in Figs.3.18, 3.20, 3.22, and 3.24. Fig. 3.25. shows the variation of the oscillation frequency with the bias current I_{B3} for the oscillator circuit no. 4 of table 3.5. Figs.3.18, 3.20, 3.22, and 3.24 show

typical waveforms generated by oscillator circuit no. 4 of table 3.3, no. 3 of table 3.4, no. 1 of table 3.5, and no. 2 of table 3.6 respectively . The performance of the circuits is thus found to be as predicted by theory.

(a) Oscillator no. 4 of table 3.3

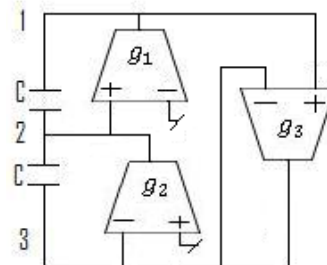The oscillator has been shown in fig.3.17

Fig. 3.17 oscillator using 3-OTA-2C

The Condition of oscillation is $(g_2 - 2g_1) = 0$ and

The frequency of oscillation is $f_o = \dfrac{1}{2\pi C}\sqrt{g_2 g_3}$

The following values of components were selected to realize a sinusoidal oscillator with a frequency of $f = 1.66kHz$, amplitude = 84 mV (P-P), $C_1 = C_2 = C = 10nF$, $I_{B1} = 6\mu A$, $I_{B2} = 13.92\mu A$, $I_{B3} = 2\mu A$ $\pm V_{CC} = \pm 9\ V\ DC$.

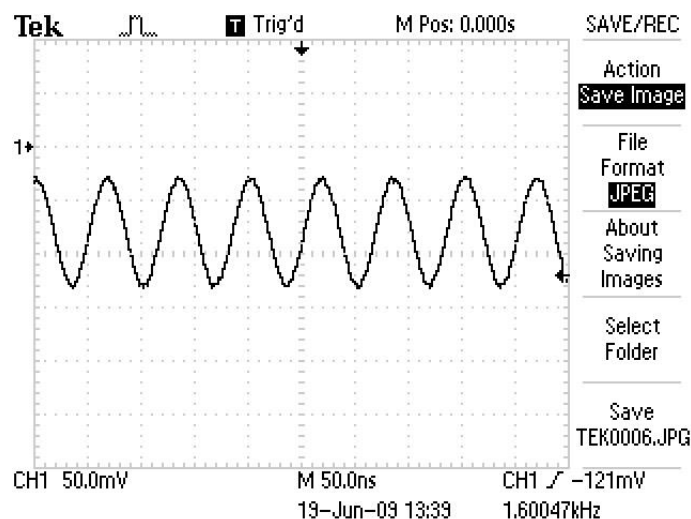The recorded output waveform is shown in Fig. 3.18.

Fig. 3.18 Output Waveform

The result closely matches with the theoretical value of frequency (1.66kHz).

(b) Oscillator no. 3 of table 3.4
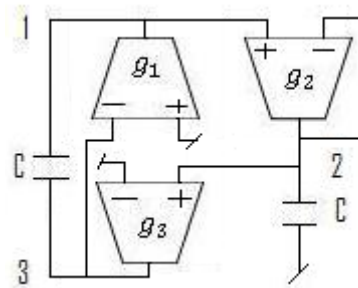
The oscillator has been shown in fig.3.19.

Fig. 3.19 oscillator using 3-OTA-2C

The Condition of oscillation is $(-g_3 + g_1) = 0$ and

The frequency of oscillation is $f_o = \frac{1}{2\pi C} \sqrt{g_2 g_3}$

The following values of components were selected to realize a sinusoidal oscillator with a frequency of $f = 2.86kHz$, amplitude = 95 mV (P-P), $C_1 = C_2 = C = 10nF$, $I_{B1} = 5\mu A$, $I_{B2} = 5\mu A$, $I_{B3} = 17\mu A$ $\pm V_{CC} = \pm 9\ V\ DC$.

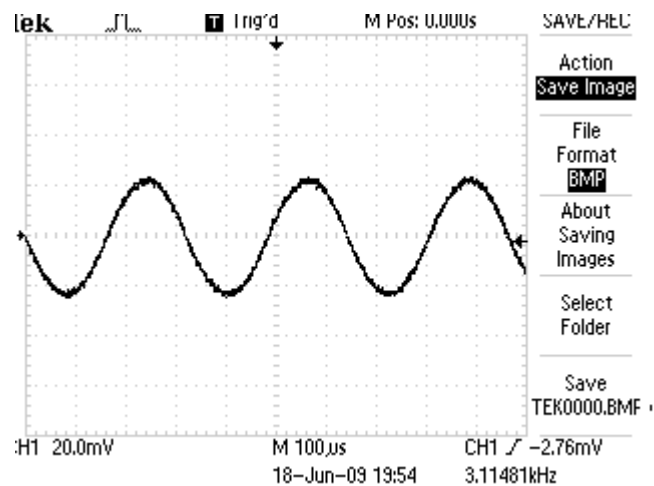The recorded output waveform is shown in Fig.3.20.

Fig. 3.20 Output Waveform

The result closely matches with the theoretical value of frequency (2.86kHz).

(c) Oscillator no. 1 of table 3.5

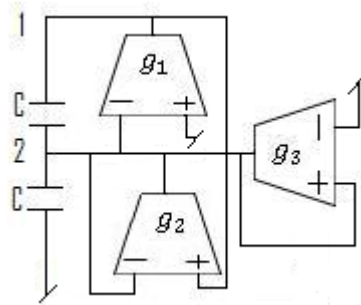The oscillator has been shown in fig.3.21.

Fig. 3.21 oscillator using 3-OTA-2C

The Condition of oscillation is $(-g_3 + g_1) = 0$ and

The frequency of oscillation is $f_o = \dfrac{1}{2\pi C}\sqrt{g_1 g_2}$

The following values of components were selected to realize a sinusoidal oscillator with a frequency of $f = 3.057 kHz$, amplitude = 48 mV (P-P), $C_1 = C_2 = C = 10nF$, $I_{B1} = 5\mu A$, $I_{B2} = 20\mu A$, $I_{B3} = 5\mu A$ $\pm V_{CC} = \pm 9\ V\ DC$.

The recorded output waveform is shown in Fig.3.22.
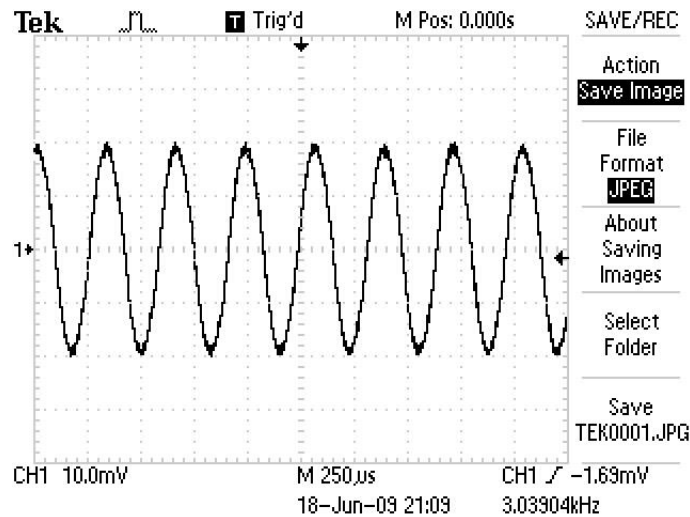

Fig. 3.22 Output Waveform

The result closely matches with the theoretical value of frequency (3.057kHz).

(d) Oscillator no. 2 of table 3.6
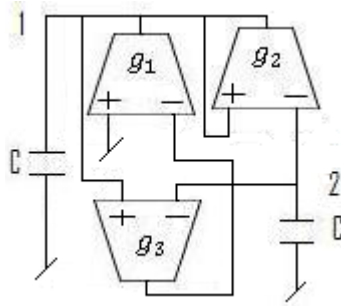
The oscillator has been shown in fig.3.23.

Fig. 3.23 oscillator using 3-OTA-2C

The Condition of oscillation is $(g_3 - g_2) = 0$ and

The frequency of oscillation is $f_o = \frac{1}{2\pi C}\sqrt{g_1 g_3}$

The following values of components were selected to realize a sinusoidal oscillator with a frequency of $f = 2.598kHz$, amplitude = 51 mV (P-P), $C_1 = C_2 = C = 10nF$, $I_{B1} = 7\mu A$, $I_{B2} = 10.32\mu A$, $I_{B3} = 10.32\mu A$ $\pm V_{CC} = \pm 9V\ DC$.

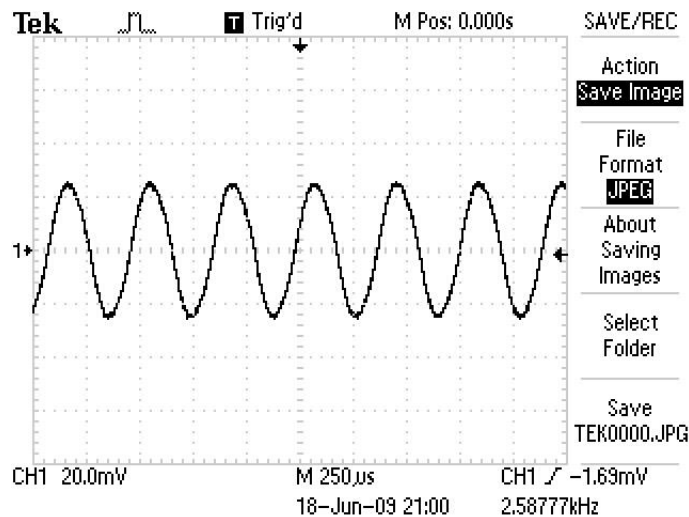The recorded output waveform is shown in Fig.3.24.

Fig. 3.24 Output Waveform

The result closely matches with the theoretical value of frequency (2.598kHz).

The Variation of the oscillation frequency with the bias current I_{B3} for the oscillator circuit no. 4 of Table 3.5 are shown in fig. 3.25. The following component Values were selected to drown this fig. $C_1 = C_2 = C = 10.45nF$, $I_{B1} = 4\mu A$, $I_{B2} = 4\mu A$, I_{B3} $Variable\ from\ 10 - 100\mu A$, $\pm V_{CC} = \pm 15\ V\ DC$.
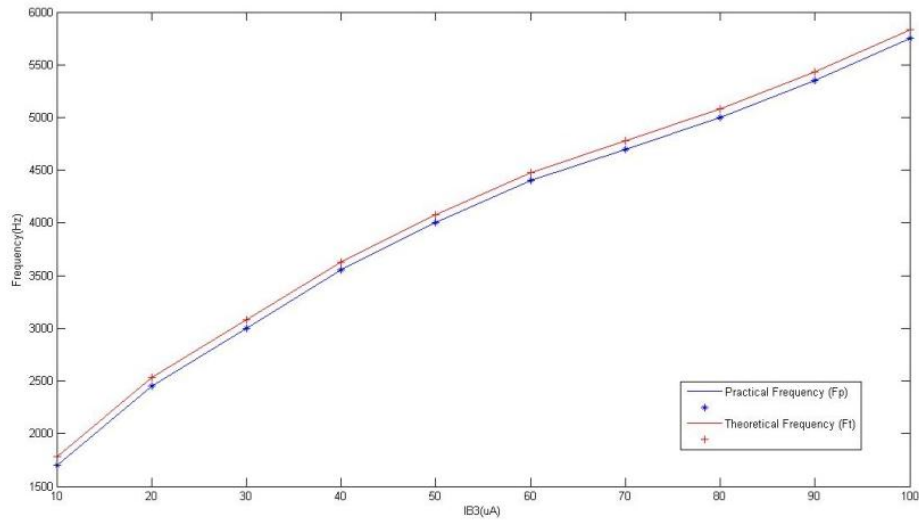

Fig. 3.25 Variation of the oscillation frequency with the bias current I_{B3} for the oscillator circuit no. 4 of Table 3.5.

3.9 CONCLUSION

In the present chapter a detailed review of some of the important works carried out on OTA-C oscillators has been presented. Some experimental results have also been given. In the next chapter we have used the methodology proposed in [7] to derive 4-OTA based sinusoidal oscillator circuits.

REFERENCES

[1] R. Senani, M. P. Tripathi and B. A. Kumar , " Systematic Generation of OTA-C Sinusoidal oscillators ", IEEE Electronics Letters , Vol. 26, No. 18, PP. 1457-1459, 30th August 1990.

[2] R. Senani, and B. Amit Kumar , " Linearly Tunable Wien Bridge oscillator Realised with OTA ", IEEE Electronics Letters , Vol. 25, No. 1, PP. 19-21, 5th January 1989.

[3] B. Linaress-Barranco, A. Rodriguez-Vazquez, J. L. Huertas and E. Sanchez-Sinencio, " Generation, design and tuning of OTA-C high-frequency sinusoidal oscillators ", IEEE Procedings-G, Vol. 139, No. 5, PP. 557-568, October 1992.

[4] M.N.S.Swamy, R.Raut and Zhigang Tang, " Generation of new OTA-C oscillator structures using network Transposition ", The 47th IEEE International Midwest Symposium on *Circuits* and Systems, PP. I-73-I-76, 5th December 1988.

[5] R. Senani, " New electronically tunable OTA-C sinusoidal oscillator ", IEEE Electronics Letters , Vol. 25, No. 4, PP. 286-287, 16th February 1989.

[6] M.T. Abuelma'atti and R. H. Almaskati, " Digitally Programmable Active-C OTA-Based Oscillator ", IEEE Transactions on Instrumentation and Measurement, Vol. 37, No. 2, June 1988.

[7] D. R. Bhaskar, M. P. Tripathi, and R. Senani, " Systematic Derivation of all Possible Canonic OTA-C Sinusoidal Oscillators ", Journal of the Franklin Institute pergamon Press Ltd., Vol. 330, No. 5, PP. 885-903, 1993.